

1 Connect Tissue Res. 2019 Mar;60(2):95-106

2 <https://doi.org/10.1080/03008207.2018.1455670>

3 **Critical-sized cartilage defects in the equine carpus**

4

5 Eve Salonius^{1*}, Lassi Rieppo^{2,3}, Mikko J. Nissi⁴, Hertta J. Pulkkinen⁵, Harold Brommer⁶, Anne
6 Brünott⁶, Tuomo S. Silvast⁷, P. René van Weeren⁶, Virpi Muhonen¹, Pieter A. J. Brama⁸, Ilkka
7 Kiviranta^{1,9}

8

9 1 Department of Orthopaedics and Traumatology, University of Helsinki, Helsinki, Finland

10 2 Research Unit of Medical Imaging, Physics and Technology, University of Oulu, Oulu,
11 Finland

12 3 Medical Research Center, University of Oulu and Oulu University Hospital, Oulu, Finland

13 4 Department of Applied Physics, University of Eastern Finland, Kuopio, Finland

14 5 Institute of Biomedicine, University of Eastern Finland, Kuopio, Finland

15 6 Department of Equine Sciences, Utrecht University, Utrecht, The Netherlands

16 7 SIB Labs, University of Eastern Finland, Kuopio, Finland.

17 8 Section of Veterinary Clinical Sciences, School of Veterinary Medicine, University College
18 Dublin, Ireland

19 9 Department of Orthopaedics and Traumatology, Helsinki University Hospital, Helsinki,
20 Finland

21

22 **Address correspondence to:* Eve Salonius, University of Helsinki, Department of Surgery,
23 Biomedicum Helsinki, Haartmaninkatu 8, 00290, Helsinki, Finland. Tel. +358-9-471-71919,
24 eve.salonius@helsinki.fi

25 *E-mail addresses:* eve.salonius@helsinki.fi (E. Salonius), lassi.riippo@oulu.fi (L. Rieppo),
26 mikko.nissi@uef.fi (M. Nissi), hertta.pulkkinen@live.com (H.J. Pulkkinen),
27 H.Brommer@uu.nl (H. Brommer), anne@brunott.biz (A. Brünott), tuomosilvast@gmail.com
28 (T.S. Silvast), r.vanweeren@uu.nl (P.R. van Weeren), virpi.muhonen@helsinki.fi (V.
29 Muhonen), pieter.brama@ucd.ie (P.A.J. Brama), ilkka.kiviranta@helsinki.fi (I. Kiviranta)

30

31 **Running title:** Critical-sized cartilage defects in the equine carpus

32

33 **Funding declaration:** This study was funded by the Academy of Finland (Grant #285909) and
34 the Finnish Funding Agency for Innovation Tekes (Grant 3344/31/03). The funding sources
35 had no role in the study design, collection, analysis and interpretation of data; in the writing of
36 the manuscript; and in the decision to submit the manuscript for publication.

37

38 **Abstract**

39 *Aim:* The horse joint, due to its similarity with the human joint, is the ultimate model for
40 translational articular cartilage repair studies. This study was designed to determine the critical
41 size of cartilage defects in the equine carpus and serve as a benchmark for the evaluation of
42 new cartilage treatment options.

43 *Materials and Methods:* Circular full-thickness cartilage defects with a diameter of 2, 4 and 8
44 mm were created in the left middle carpal joint and similar osteochondral (3.5 mm in depth)
45 defects in the right middle carpal joint of five horses. Spontaneously formed repair tissue was
46 examined macroscopically, with MR and μ CT imaging, polarized light microscopy, standard
47 histology and immunohistochemistry at 12 months.

48 *Results:* Filling of 2 mm chondral defects was good ($77.8\pm 8.5\%$) but proteoglycan depletion
49 was evident in Safranin-O staining and gadolinium-enhanced MRI (T_{1Gd}). Larger chondral
50 defects showed poor filling ($50.6\pm 2.7\%$ in 4 mm and $31.9\pm 7.3\%$ in 8 mm defects). Lesion filling
51 in 2, 4 and 8 mm osteochondral defects was $82.3\pm 3.0\%$, $68.0\pm 4.6\%$ and $70.8\pm 15.4\%$,
52 respectively. Type II collagen staining was seen in 9/15 osteochondral defects but only in 1/15
53 chondral defects. Subchondral bone pathologies were evident in 14/15 osteochondral samples
54 but only in 5/15 chondral samples. Although osteochondral lesions showed better neotissue
55 quality than chondral lesions, the overall repair was deemed unsatisfactory because of the
56 subchondral bone pathologies.

57 *Conclusions:* We recommend classifying 4 mm as critical osteochondral lesion size and 2 mm
58 as critical chondral lesion size for cartilage repair research in the equine carpal joint model.

59 **Keywords:** cartilage repair; animal model; spontaneous repair; preclinical research; critical-
60 sized defect

61 **Introduction**

62 Animal models are used for the evaluation of the efficacy of new surgical techniques. When
63 investigating articular cartilage repair *in vivo*, joint size and cartilage thickness are considered
64 key factors in defining the most appropriate species. (1,2) The joint size, cartilage thickness and
65 gait mechanics of the horse are closest to those of humans. (3,4) Moreover, naturally occurring
66 equine cartilage lesions have similar etiology as human lesions. (1,3,4) These similarities allow
67 for a realistic evaluation of novel methods for cartilage repair. In the equine model, stifle,
68 tarsotibial and carpal joints have been used in translational cartilage repair research. To enable
69 effective use of the equine model in translational cartilage research, the intrinsic repair capacity
70 of equine cartilage in the specific joint must be known.

71 A critical-sized lesion is a lesion of a size beyond which the defect does not heal spontaneously.
72 Knowledge about critical lesion sizes in animal experiments is necessary for cost reduction and
73 minimizing the suffering of animals while still providing reliable data on the effect of the
74 studied technique. Critical lesion size used in previous equine studies has been defined as lesion
75 size beyond which any void made is not filled. (5) However, tissue quality should also be taken
76 into consideration when defining cartilage repair. Aiming at tissue regeneration, *i.e.* restoration
77 of normal tissue architecture and function, instead of merely filling the defects is paramount for
78 achieving durable results. (6) Therefore, this kind of defect filling cannot be considered to be
79 successful healing.

80 There are no recent studies on spontaneous cartilage repair in the equine carpus, and previous
81 studies have generally used basic methods, such as macroscopic inspection, standard histology
82 and basic biochemistry for the assessment of repair tissue quantity and quality. (5,7) Apart from

83 this, to our knowledge, there are no data on the long-term evolution of artificially made
84 superficial chondral lesions in horses. Given the increasing recognition of the equine model for
85 the evaluation of cartilage repair techniques, (1,3,8) and the equine carpus being the most
86 common site of naturally occurring osteoarthritis after metacarpophalangeal joint, (9) our study
87 focused on characterization of the long-term spontaneous repair of variably sized chondral and
88 osteochondral defects in the equine carpus using state-of-the-art analytical techniques. As small
89 cartilage defects have been thought to heal well, (3,5,8) we hypothesized that the critical defect
90 size would be larger than 2 mm in diameter. The information obtained in this study can be used
91 as a benchmark when evaluating the effect of different techniques aiming at cartilage
92 regeneration in an equine translational model, as it defines to what extent lesions of different
93 sizes will heal spontaneously over a long period (12 months) in the equine carpus.

94

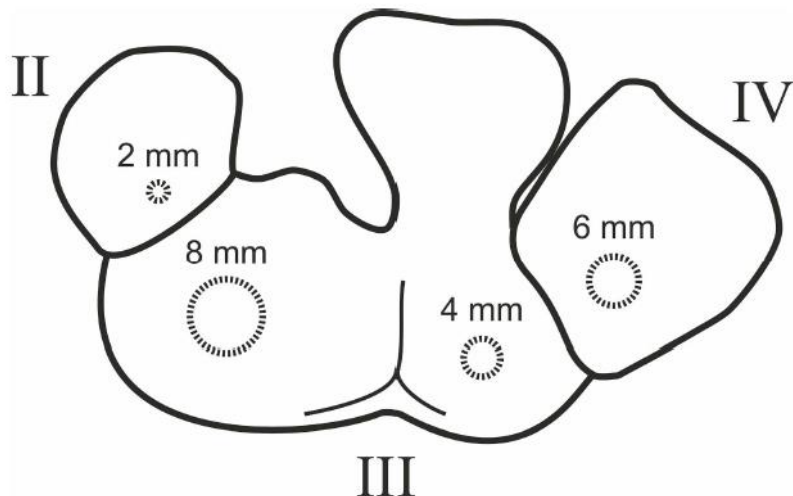
95 **Methods**

96 *Surgical procedure*

97 Five 24-month-old horses (*Equus caballus*) were included in this study. The study was
98 authorized by the Utrecht University Animal Experiments Committee (0412.0601, Utrecht, The
99 Netherlands) in compliance with the Dutch Act on Animal Experimentation. The animal care
100 was in accordance with Utrecht University guidelines. Surgery was performed under general
101 anesthesia following routine clinical procedures. All the horses were assessed clinically and
102 radiologically prior to inclusion in the study and were found to be skeletally mature and to
103 present no abnormalities.

104 The horses received meloxicam pre-operatively (0.6 mg/kg, *i.v.*, Metacam®, Boehringer
105 Ingelheim). The middle carpal joints were approached through a lateral-dorsal and medio-
106 dorsal 1.5–2 cm length arthrotomy to create defects of 2 mm (3 mm²), 4 mm (13 mm²), 6 mm
107 (28 mm²) and 8 mm (50 mm²) in diameter on the 2nd, 3rd and 4th carpal bones as shown in Figure
108 1. Defects were pre-punched with a 2, 4, 6 or 8 mm skin biopsy punch. For chondral defects,
109 cartilage was carefully removed with ring curettes onto the level of calcified cartilage
110 (approximately 1 mm in depth) in the left carpus. For osteochondral lesions created in the right
111 carpus, drilling was performed under continuous lavage with Ringer's solution using a hand
112 drill. A 2, 4, 6 or 8 mm pointed drill bit was initially used, followed by a custom-made flattened
113 drill bit of the same size and a custom-made drill sleeve to provide a uniform defect with a
114 flattened bottom and controlled depth of 3.5 mm. Healthy cartilage adjacent to the lesions
115 served as control for all defects.

116



117

118 **Figure 1.** Schematic drawing of the left equine carpal bones II-IV with the four different lesion sizes marked with
119 dashed lines.

120

121 Post-operatively, the animals were confined to individual box-stalls (3.5×3.5m) for two weeks,
122 after which a gradual six-week rehabilitation program consisting of incremental controlled
123 walking started. Thereafter, depending on the season and weather conditions, the animals were
124 turned out to pasture or kept in box stalls with daily exercise of 20-30 minutes in a mechanical
125 horse walker. The exercise regimen was identical for all horses. Synovial fluid and blood
126 samples were collected at weeks 0, 2, 6, 14, 26, 38 and immediately after euthanasia. The total
127 follow-up period was 12 months during which the lesions were allowed to heal spontaneously.

128 The 6 mm lesions created in *os carpale IV* were used in other studies. (10-12) As their
129 processing was different from the other samples, the 6 mm lesions are not included in this study.

130

131

132 ***Macroscopic evaluation and sample collection***

133 After sacrificing the animals, the carpal joints were opened and macroscopic photographs were
134 taken. Cylindrical osteochondral samples (14 mm in diameter and approximately 1 cm in depth)
135 were taken using a hollow drill that was centered over the original lesion. The samples were
136 frozen and stored at -20°C until further processing.

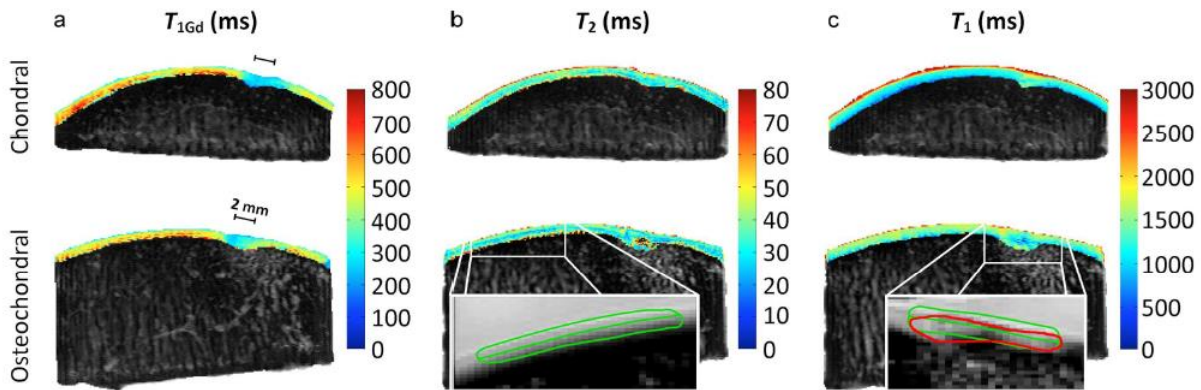
137 ***Micro-computed tomography (μCT)***

138 The samples were thawed in PBS supplemented with inhibitors of metalloproteinases [5 mM
139 ethylenediamine tetraacetic acid (EDTA) disodium salt (VWR International, Fontenay, France)
140 and 5 mM benzamidine hydrochloride (Sigma-Aldrich, St. Louis, MO)], and analyzed with a
141 SkyScan-1172 scanner (SkyScan, Aartselaar, Belgium). The volume of interest was a cylinder
142 with the diameter of the defect size and height of 6 mm. In control samples, the diameter was
143 8 mm. The data was analyzed for the structural bone parameters: bone volume fraction (BV/TV),
144 trabecular thickness ($Tb.Th$), trabecular spacing ($Tb.Sp$), and trabecular number ($Tb.N$).

145 ***Magnetic resonance imaging (MRI)***

146 Thawed samples were MR imaged with a 9.4 T device (Oxford 400 NMR vertical magnet;
147 Oxford Instruments, Witney, England), equipped with a Varian DirectDrive console (VnmrJ
148 2.3, Varian, Palo Alto, CA, USA) and a 19 mm quadrature volume coil (RAPID Biomedical,
149 Rimpar, Germany). The specimens were placed in a test tube and immersed in saline. T_2
150 relaxation time was measured in a single slice of 1 mm thickness using a single echo spin echo
151 sequence with TEs of 12, 24, 50, 80 and 110 ms, a TR of 2.5 s and in-plane resolution of 70 x
152 140 μm . Native T_1 relaxation time was measured in the same slice with the same resolution,
153 using a progressive saturation recovery sequence with TRs of 0.3, 0.6, 1.2, 2.4 and 4.8 s and

154 TE of 11.7 ms. After the first scans, the specimens were immersed in a 1.0 mM Gd-DTPA²⁻
 155 solution for 20 hours at room temperature (RT), after which T_{1Gd} was measured using the same
 156 saturation recovery sequence with the same resolution, but with TRs of 0.1, 0.2, 0.4, 0.8 and
 157 1.6 s. Two regions of interest (ROIs) were defined in the MR images as exemplified in Figure
 158 2: ROI 1 covered exclusively any repair tissue at the lesion sites of the samples, regardless of
 159 its location (repair tissue only). ROI 2 was spatially aligned with the surrounding healthy
 160 cartilage and located where the repair tissue assumingly should be if everything was perfectly
 161 healed, and further split into superficial and deep halves (upper and lower part of the cartilage).
 162 A control ROI was defined in the adjacent healthy tissue and also split into superficial and deep
 163 halves.



164
 165 **Figure 2.** Representative MRI relaxation time maps of the chondral (top row) and osteochondral (bottom row)
 166 lesions of 2 mm diameter. Lesion site is immediately below the scale bar (2 mm). Shorter T_{1Gd} relaxation times
 167 were observed in both lesions, but more prominently so in the chondral lesion (a). Slight differences as compared
 168 to the adjacent tissue were also evident in the T_2 and T_1 relaxation time maps (a, b). The ROI for control tissue is
 169 exemplified in the magnification of b. In the magnification of c, the ROI 1 for the repair tissue is marked with red,
 170 and the ROI 2 aligned to adjacent healthy cartilage is marked with green.

171

172 ***Polarized light microscopy***

173 After the imaging studies, the samples were processed for histology. The sample cylinders were
174 fixed in 10% formalin for 48 hours at RT. The samples were decalcified in 10% EDTA and 4%
175 formaldehyde in 0.1 M phosphate buffer at RT, cut in half, dehydrated in ascending alcohol
176 series, and embedded in paraffin. Tissue sections of 5 μm in thickness were cut from the middle
177 of the lesion.

178 Unstained tissue sections were measured using polarized light microscopy (Leitz Ortholux II
179 POL, Leitz Wezlar, Wezlar, Germany). (13) The repair tissue was evaluated using a 300- μm -
180 wide ROI, which was divided into ten layers of equal thicknesses for the analysis. The
181 orientation of collagen fibrils in relation to the cartilage surface (0–90 degrees), and parallelism
182 index (PI), which describes the randomness of fibril orientations within the pixel (0–1, where
183 0 indicates completely random organization and 1 indicates completely parallel organization),
184 (13) were determined from the most superficial, middle and the deepest section.

185 ***Histological and immunohistological evaluation***

186 Tissue sections were stained with Safranin-O using standard protocols. (14) Mosaic images of
187 the histological sections were generated with the Zeiss AxioImager Z1 microscope system
188 equipped with an AxioCam MRc5 camera and Zen blue edition software (Carl Zeiss
189 Microscopy GmbH).

190 Lesion filling was calculated from the Safranin-O stained sections using color thresholding in
191 the Fiji program. (15) The ROI from which the lesion filling was calculated covered the entire
192 lesion, with the width being the defect diameter and the depth being 1 mm for chondral lesions
193 and 3.5 mm for osteochondral lesions. As the ROI for the osteochondral defects extended into

194 the subchondral bone, the natural trabecular spaces in the sections resulted in empty spaces and
195 thus in a smaller filling degree in the healthy osteochondral control samples than in the chondral
196 samples.

197 The Safranin-O stained tissue sections in study III were evaluated using the OARSI
198 histopathology score validated for equine cartilage, in which each parameter is evaluated 0–4
199 where 0 represents healthy cartilage tissue.(16) The sections were scored by three independent,
200 blinded observers and an average of the scores was used. The defects that lacked any repair
201 tissue were given the worst score of 4 for each parameter.

202 A previously published protocol (14) was used to evaluate the staining for type I and type II
203 collagen. Briefly, the sections were digested with hyaluronidase (2 mg/ml, Sigma-Aldrich) and
204 pronase (2 mg/ml, Calbiochem, Merck KGaA), and immersed in hydrogen peroxide
205 (EnVision®+ System-HRP (AEC), Dako North America Inc.) to block endogenous peroxidase
206 activity. Non-specific staining was blocked with 10% normal goat serum (Dako Denmark A/S,
207 Glostrup, Denmark). The sections were then incubated overnight at 4°C with primary
208 antibodies against collagen type II (ab34712, Abcam) and collagen type I (ab34710), and
209 diluted to 4 µg/ml with PBS supplemented with 1% bovine serum albumin (Sigma-Aldrich).
210 Horseradish peroxidase (HRP)-conjugated goat anti-rabbit secondary antibody (Dako) was then
211 applied. Antibody binding was visualized with AEC substrate chromogen (Dako). The staining
212 of each sample was evaluated under light microscopy.

213 *Statistical analysis*

214 Confidence intervals and standard errors were calculated with the IBM SPSS Statistics 22
215 software. Osteochondral and chondral lesions of the same diameter were compared to each

216 other. The significances of differences in the μ CT, MRI and polarized light microscopy
217 parameters were evaluated with a pairwise t test, and Sidak adjustment was made for multiple
218 testing. Significances of difference in lesion filling was calculated with permutation type
219 ANOVA testing and Sidak adjustment. Comparisons of lesions and control tissue were made
220 with permutation type ANOVA testing with Dunnet method. A p value under 0.05 was used as
221 the threshold to indicate a statistically significant difference.

222

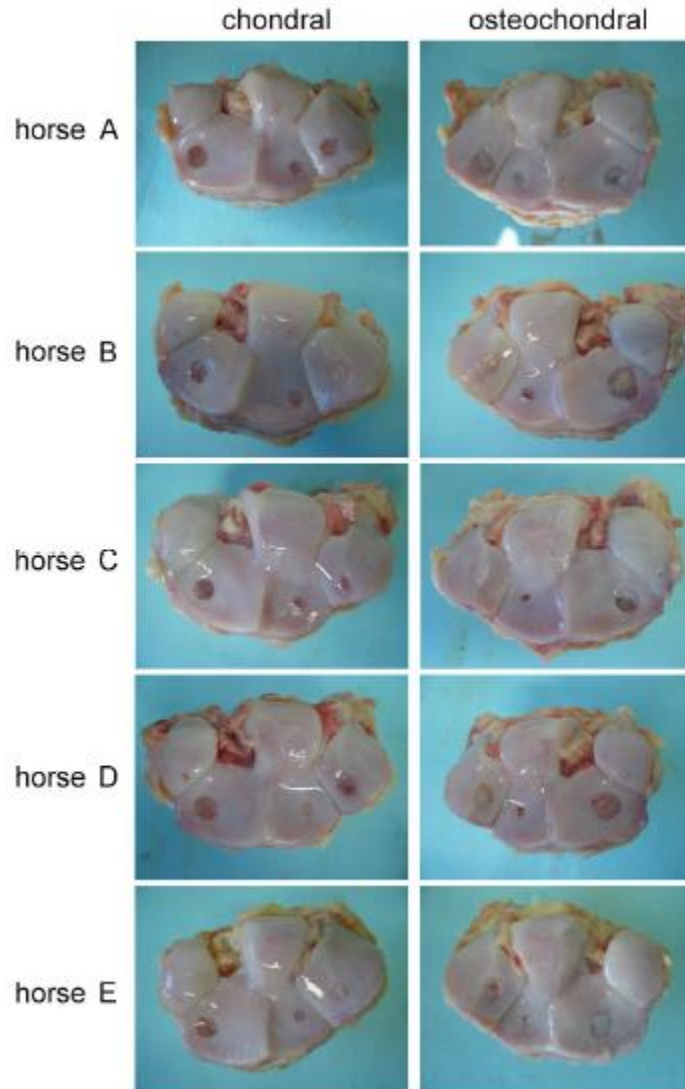
223 **Results**

224 *Post-operative animal wellbeing*

225 The surgeries were uneventful and all animals recovered well. All the horses demonstrated a
226 pattern of decreasing joint effusion and lameness after surgery that can be expected during the
227 normal healing of an arthrotomy in clinical cases. Joint effusion and lameness were minimal at
228 postoperative day 10 during suture removal and all the horses were fully recovered by 3-4
229 weeks post-surgery. No clinical abnormalities were noticed in any of the horses during the
230 remainder of the experiment.

231 *Gross appearance of the repair tissue*

232 Most of the 2 mm lesions showed good macroscopic filling (5 of 5 osteochondral and 3 of 5
233 chondral defects) (Figure 3). The 4 mm lesions were clearly distinguishable from the
234 surrounding healthy cartilage and were incompletely filled. One chondral 4 mm lesion (animal
235 D) showed rather good filling. Each of the 8 mm lesions was incompletely filled. No
236 degenerative changes were detected.



237

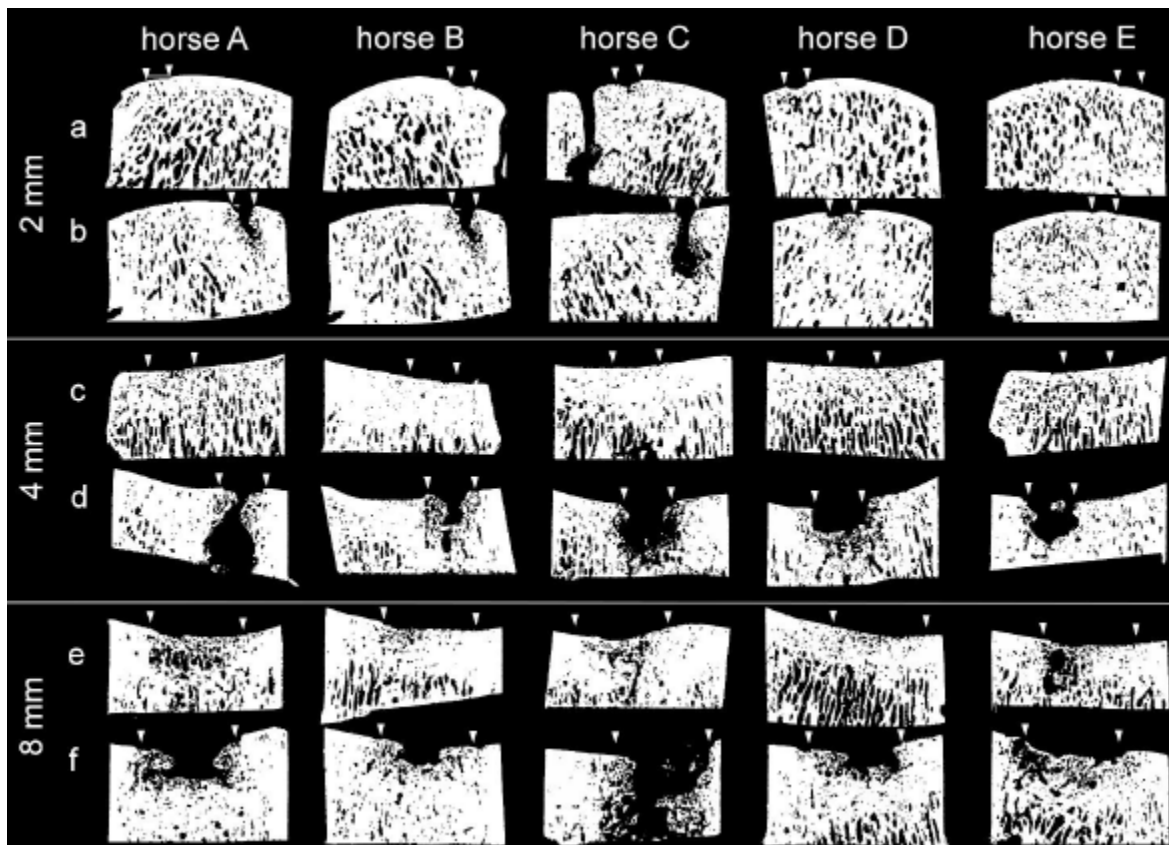
238 **Figure 3.** Photographs of the joints taken directly after sacrificing the animals. Chondral lesions are in the left
239 column and osteochondral in the right column. Each horse is represented in its own row. Macroscopically, 5 of 5
240 osteochondral and 3 of 5 chondral lesions with the diameter of 2 mm were filled with repair tissue. Of the 4 mm
241 lesions, only one chondral lesion (horse D) was well filled, the other lesions were easily distinguishable and not
242 filled to the level of the surrounding cartilage. Each 8 mm defect was clearly visible but one osteochondral defect
243 (horse E) showed good filling in the middle of the lesion.

244

245

246 ***Micro-computed tomography***

247 Visually, the bone structure was normal under the chondral lesions of 2 mm and 4 mm in
248 diameter (Figure 4). Bone compactness was visually observed to be decreased in 4 of the 5
249 chondral lesions with a diameter of 8 mm, and one of these samples showed a small subchondral
250 bone erosion. There were subchondral bone changes in all but one of the osteochondral defects
251 (the exception being horse E, 2 mm lesion). Only two osteochondral samples with a diameter
252 of 2 mm presented without cyst-like bone changes. All osteochondral lesions of 4 mm and 8
253 mm in diameter had unhealed bone or a cyst-like bone lesion. There were no clear trends in the
254 numeral μ CT data and the individual variation between the samples was large. No statistically
255 significant differences were found between the chondral and osteochondral defects but the
256 trabeculae were thinner in osteochondral defects of all sizes than in healthy control tissue
257 ($p=0.003$).



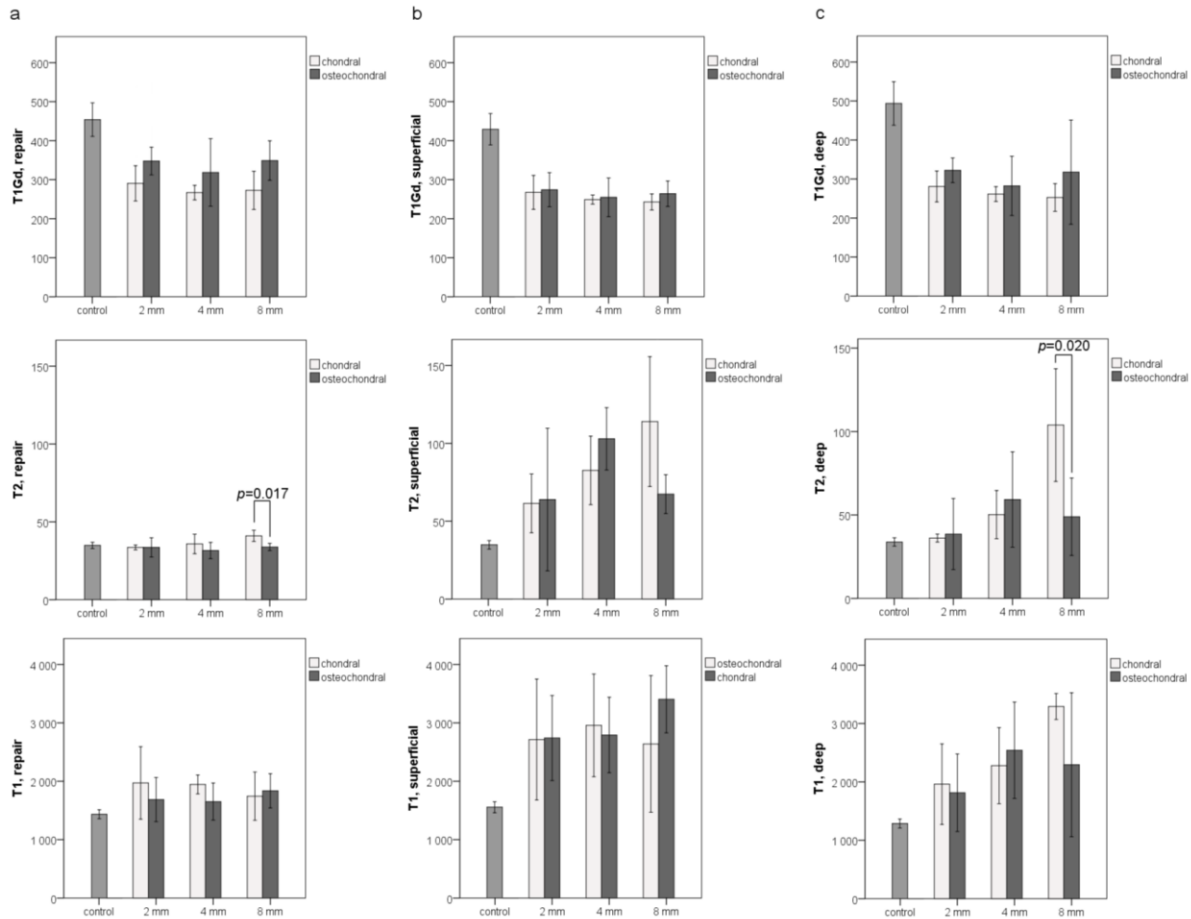
258

259 **Figure 4.** Micro-computational tomographic image of the middle part of each specimen. The osteochondral lesions
260 (b, d, f) presented with subchondral bone resorption, whereas the bone structure in the chondral lesions (a, c, e)
261 was either undisturbed or slightly decreased in density. Arrowheads show the site of the original defect.

262

263 ***Magnetic resonance imaging***

264 The relaxation times in ROI 1 (repair tissue only) showed no clear trends with respect to the
265 increasing lesion diameter (Figure 5a). However, T_{1Gd} relaxation times were shorter ($p=0.014$
266 and $p<0.001$ for osteochondral and chondral lesions, respectively) and T_1 relaxation times
267 slightly longer ($p=0.156$ and $p=0.037$ for osteochondral and chondral lesions, respectively) in
268 the repair tissues than in the control samples (Figure 5).



269

270 **Figure 5.** Mean relaxation time values (ms) of the magnetic resonance imaging in the different cartilage ROIs.
 271 Results for the repair tissue only (ROI 1) in each group are shown in (a), and the area aligned to the adjacent
 272 healthy cartilage (ROI 2) was divided into a superficial half (b) and deep half (c). Chondral lesions are colored
 273 white and osteochondral ones dark gray. The whiskers represent 95% confidence interval. Statistically significant
 274 p values are marked in the images.

275 In all ROIs, the osteochondral lesions had longer T_{1Gd} relaxation times than the chondral lesions,
 276 indicative of a higher proteoglycan content. However, no statistically significant differences
 277 were observed. In ROI 1, the T_2 relaxation time was shorter in the 8 mm wide osteochondral
 278 defects than in the chondral defects (33.8 ± 0.8 ms for osteochondral and 41.0 ± 1.3 ms for
 279 chondral lesions, $p=0.020$). ROI 2 (lesion area aligned to adjacent healthy cartilage) showed

280 increasing T_2 s with larger lesion diameters and towards the cartilage surface. Osteochondral
281 lesions with a diameter of 8 mm deviated from this trend and showed lower T_2 values (48.9 ± 8.4
282 ms) than the 4 mm lesions (59.2 ± 10.3 ms). The 8 mm lesions also demonstrated a significant
283 difference between the osteochondral and chondral samples in the deep part of ROI 2
284 (103.9 ± 12.2 ms for chondral and 48.9 ± 8.4 ms for osteochondral defects, respectively,
285 $p=0.020$).

286 The T_1 relaxation time of the chondral samples in ROI 2 showed a trend of increasing with
287 lesion diameter and from the deep part of the tissue towards the cartilage surface (Figure 5b
288 and c). The T_1 relaxation times of all chondral lesions were higher than those of the control
289 tissue ($p<0.001$). The largest variation in T_1 relaxation time was noted for osteochondral lesions
290 with a diameter of 8 mm. T_1 relaxation time did not show significant differences between the
291 groups in either of the ROIs.

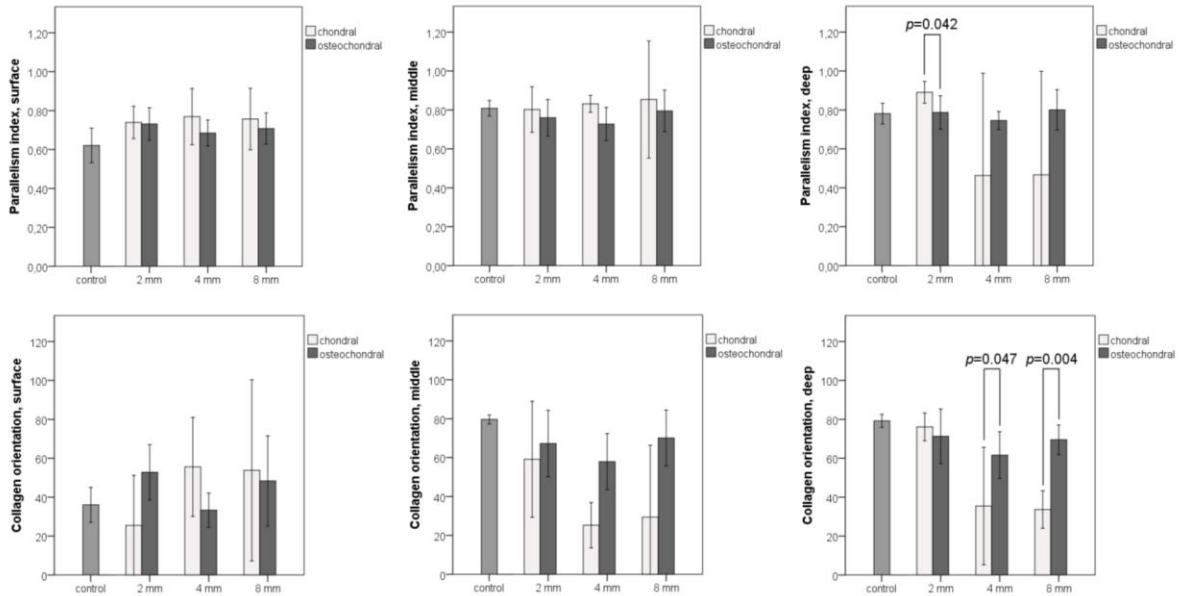
292 Changes in the relaxation times were visually observed, especially in the T_{1Ga} relaxation time
293 between the lesion sites and adjacent tissue, exemplified here in the cases of the 2 mm lesions
294 (Figure 2). While the relaxation times of the subchondral bone are not shown, also differences
295 in the MRI signal of the subchondral bone immediately below the lesion site were observed
296 between the lesion types: a uniform appearance of the signal is seen below the chondral lesions,
297 while an area of increased signal was present in the vicinity of the osteochondral lesions,
298 indicating an increased water content in the area (Figure 2).

299 ***Polarized light microscopy***

300 Polarized light microscopy showed high parallelism indexes (PI) in all samples (Figure 6).
301 Chondral lesions with a diameter of 2 mm showed a higher parallelism of collagen fibrils than

302 osteochondral lesions in the deep part of the repair tissue (0.891 ± 0.02 for chondral and
 303 0.787 ± 0.03 for osteochondral lesions, $p=0.042$). Otherwise, no statistically significant
 304 differences in the PI between the lesion diameters or the lesion depths were detected.

305



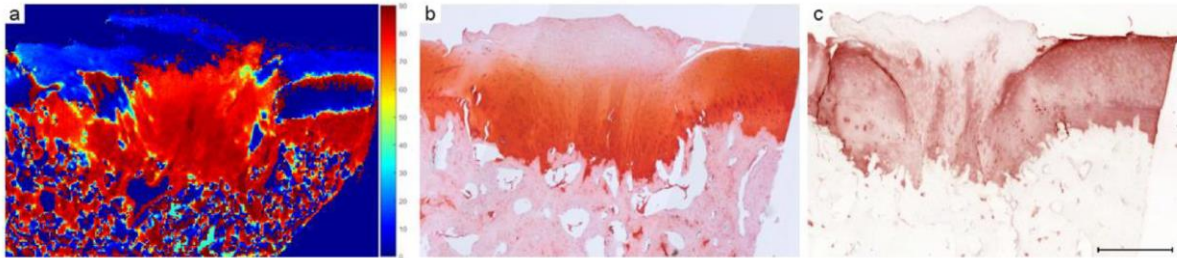
306

307 **Figure 6.** Bar diagrams showing the mean parallelism index (PI, top row) of the collagen fibrils and the mean
 308 orientation (bottom row) of the fibrils. Chondral lesions are colored white and osteochondral lesions dark gray.
 309 The whiskers represent 95% confidence interval. Statistically significant p values are marked in the images.

310

311 Collagen orientation showed large variations between the groups and between individual
 312 samples. Collagen orientation changed toward the typical tangential orientation in the
 313 superficial part of the 2 mm lesions (Figure 7a) and deviated from what was expected in the
 314 larger lesions. The osteochondral samples showed a higher level of fibril organization than the
 315 chondral samples in the deep part of the tissue, the collagen orientation being $61.6\pm 4.3^\circ$ for 4

316 mm and $69.5 \pm 2.7^\circ$ for 8 mm osteochondral defects, and $35.4 \pm 7.0^\circ$ for 4 mm and $33.6 \pm 2.2^\circ$ for
317 8 mm chondral defects ($p=0.047$ and $p=0.004$ for 4 mm and 8 mm lesions, respectively).



318

319 **Figure 7.** Representative osteochondral defect with a diameter of 2 mm. a) Polarized light microscopy showed the
320 change in collagen orientation toward the typical tangential orientation in the superficial layer. b) Safranin-O
321 staining showed good filling and abundant proteoglycans in the deep part of the repaired cartilage tissue. c)
322 Immunohistochemical staining for type II collagen. Scale bar:500 μ m.

323

324 *Histological repair quality*

325 Lesion filling was analyzed from the Safranin-O stained sections. Filling of the osteochondral
326 control samples was $81.7 \pm 0.2\%$ and filling of chondral controls was $99.4 \pm 4.7\%$. Lesion filling
327 was most complete ($82.3 \pm 3.0\%$) in the osteochondral lesions in which the repair tissue reached
328 the level of the surrounding cartilage surface in all of the 2 mm lesions (Figure 7, Figure 8). On
329 the other hand, 4 of 5 of the 4 mm lesions and 1 of 5 of the 8 mm lesions presented with repair
330 tissue non-aligned with the surrounding cartilage with filling of $68.0 \pm 4.6\%$ for 4 mm
331 osteochondral defects and $70.8 \pm 15.4\%$ for 8 mm defects, respectively. All of the 2 mm chondral
332 lesions showed good lesion filling ($77.8 \pm 8.5\%$) whereas filling of the 4 mm chondral defects
333 was $50.6 \pm 2.7\%$ and filling of the 8 mm defects was $31.9 \pm 7.3\%$. 9 of 10 of the 4 mm and 8 mm
334 lesions showed only small islands of unstained repair tissue or even a complete absence of

335 repair cartilage in the histological sections. Islands of repair tissue occurred at sites where the
336 subchondral bone plate was disrupted (Figure 8). None of the defects showed lateral expansion.
337 The filling of osteochondral samples did not differ from healthy control cartilage ($p=0.085$)
338 whereas the filling of the chondral samples differed from the controls ($p<0.001$).

339 More than half of the osteochondral lesions in each diameter category showed repair tissue with
340 good Safranin-O stain uptake whereas only one of the chondral lesions showed Safranin-O
341 positive tissue at the repair site (Table 2). As the repair tissue was absent from two 4 mm
342 chondral lesion and four 8 mm chondral lesion samples, those samples were perceived negative
343 for Safranin-O uptake. Typically, the osteochondral samples showed hyaline-like cartilage in
344 the deep or middle part of the repair tissue and fibrous tissue on the surface. The best and the
345 worst repairs in each group are shown in Figure 8.

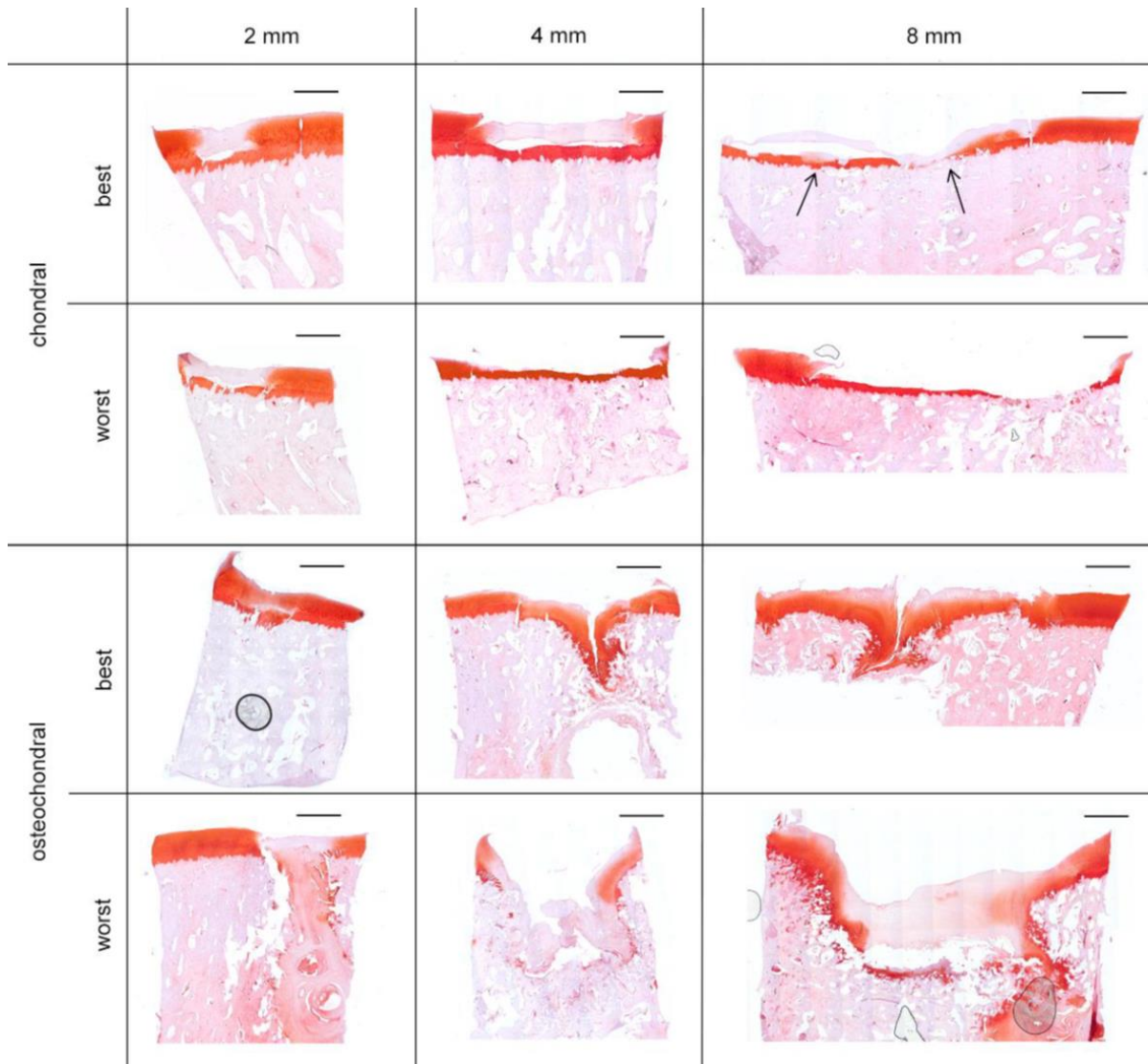
346 Typically, osteochondral defects showed lower values of OARSI score than chondral defects
347 (Table 1). This is indicative of better tissue quality in the osteochondral samples. Loss of
348 Safranin-O uptake was common in all of the defect sizes. No degenerative changes were
349 detected in the control cartilage adjacent to the lesions.

350 ***Immunohistochemistry***

351 Almost all of the 2 mm osteochondral samples (4 of 5) showed positive type II collagen staining
352 and only one of these samples showed positive type I collagen staining (Figure 7, Table 2). In
353 the 2 mm chondral samples, positive staining for type II and type I collagen was shown in 1 of
354 5 and 4 of 5 samples, respectively. Fibrocartilage formation was evident in the larger chondral
355 and osteochondral lesions where a mixture of type I and type II collagen positive tissue was

356 present. Since the repair tissue was detached from two of the 4 mm chondral lesions and four
357 of the 8 mm chondral lesions, these were perceived negative for both type I and II collagen.

358



359

360 **Figure 8.** The best and worst Safranin-O stained histological section in each study group. Repair tissue seemed to
361 originate partly from the subchondral bone at the sites where the calcified cartilage was disrupted (arrows). Scale
362 bars: 1 mm.

363 **Table 1.** Results of the OARSI microscopic scoring system (16) for each study group. Each parameter was
 364 evaluated 0–4 where 0 represents healthy cartilage tissue. The values are presented as mean \pm standard error (SE).

	Chondrocyte necrosis	Cluster formation	Fibrillation / fissuring	Focal cell loss	Loss of Safranin-O
Chondral					
Control	0.84 \pm 0.13	0.80 \pm 0.12	0.13 \pm 0.05	0.00 \pm 0.00	0.07 \pm 0.04
2 mm	0.55 \pm 0.16	0.36 \pm 0.14	1.36 \pm 0.15	1.76 \pm 0.19	3.76 \pm 0.11
4 mm	3.72 \pm 0.14	3.11 \pm 0.27	3.14 \pm 0.26	3.47 \pm 0.17	4.00 \pm 0.00
8 mm	2.91 \pm 0.24	2.53 \pm 0.28	3.16 \pm 0.20	3.02 \pm 0.21	3.91 \pm 0.04
Osteochondral					
Control	0.24 \pm 0.08	0.53 \pm 0.10	1.16 \pm 0.12	0.07 \pm 0.04	0.22 \pm 0.06
2 mm	1.51 \pm 0.20	0.71 \pm 0.12	1.29 \pm 0.15	1.29 \pm 0.16	2.02 \pm 0.20
4 mm	2.22 \pm 0.21	1.37 \pm 0.19	2.15 \pm 0.14	2.22 \pm 0.16	3.35 \pm 0.11
8 mm	0.59 \pm 0.11	0.47 \pm 0.11	1.69 \pm 0.16	1.24 \pm 0.13	3.25 \pm 0.10

365

366 **Table 2.** Number of specimens with positive staining for Safranin-O or immunohistochemical staining for type I
 367 and type II collagen in each lesion type. As the repair tissue was detached from two of the 4 mm chondral lesions
 368 and four of the 8 mm chondral lesions, those samples were perceived negative for Safranin-O and type I and II
 369 collagen.

	2 mm		4 mm		8 mm	
	Chondral	Osteochondral	Chondral	Osteochondral	Chondral	Osteochondral
Safranin-O	1/5	4/5	0/5	4/5	0/5	3/5
Type I collagen	4/5	1/5	2/5	2/5	1/5	2/5
Type II collagen	1/5	4/5	0/5	2/5	0/5	3/5

370

371 **Discussion**

372 The purpose of this study was to determine the intrinsic repair capacity of equine carpal articular
373 cartilage to set a benchmark for studies evaluating articular cartilage repair strategies using the
374 equine carpus as a model. Knowledge on spontaneous repair capacity and critical lesion size
375 improves cost-effectiveness and minimizes animal suffering in animal experiments. The quality
376 and quantity of the repair tissue in both chondral and osteochondral defects were evaluated in
377 this study. Complete tissue regeneration was not achieved as the repair tissue structure differed
378 from healthy cartilage in all the defects. Only the osteochondral lesions with 2 mm diameter
379 showed good Safranin-O staining indicating a good quality of the repair tissue, while equally
380 sized chondral defects failed to spontaneously repair to hyaline cartilage. Chondral defects and
381 osteochondral defects with the diameter of 4 mm and 8 mm showed depletion of proteoglycans
382 and structural disorganization.

383 The healing of equine carpal cartilage defects was first described by Riddle (17) who created
384 superficial and full-thickness defects in the carpus of four horses (150 mm²) and six ponies (100
385 mm²). He concluded that the superficial defects did not heal past the 8-month time point and
386 that in order for the defects to heal, they should reach the subchondral bone. The importance of
387 the connection to the bone marrow spaces has since been confirmed by others. (18,19) Mean
388 filling of both untreated and microfracture-treated chondral defects of 100 mm² in equine carpus
389 in the study by Frisbie was, however, only 65% or less. (18)

390 In a study evaluating spontaneous healing of full-thickness cartilage defects in the equine carpus
391 by Hurtig et al., (5) lesions with a surface area of 5 mm² were filled with fibrocartilaginous
392 repair tissue but lesions of 15 mm² deteriorated to dense fibrous tissue. This is corroborated by

393 our study, where nearly all full-thickness chondral defects of 3 mm² (2 mm in diameter) showed
394 fibrocartilaginous repair, and larger defects presented with incomplete fibrocartilage covering
395 or no repair tissue at all.

396 Spontaneous defect healing reported in previous equine studies is mainly described as filling of
397 the lesions or formation of fibrous tissue and fibrocartilage. (5,20) Fibrocartilage, however, has
398 lower mechanical strength than hyaline cartilage and as such, it is more prone to wearing out.
399 (21) Durable, long-lasting results can only be achieved by restoration of fully functional hyaline
400 cartilage. (6) The focus of interventions aiming at cartilage repair has shifted from simply filling
401 the lesions to restoring mature hyaline cartilage. In order to reliably determine the critical lesion
402 size, it is paramount to evaluate both the quantity and quality of repair tissue. In the present
403 study, only the osteochondral defects showed hyaline-like repair tissue with higher
404 proteoglycan content and better filling after a 12-month follow-up (Figure 4, Figure 8). Even
405 though small full-thickness chondral defects have been thought to heal spontaneously (3,5,8),
406 the results of this study suggest otherwise. Although the filling in the 2 mm defects was good
407 macroscopically, depletion of proteoglycans was evident both in Safranin-O staining and
408 gadolinium-enhanced MR imaging (T_{1Gd}). Structural disorganization and fibrocartilage
409 formation were seen in polarized light microscopy and as a mixture of type I and II collagen
410 staining in immunohistochemistry, and low T_2 and T_{1Gd} values in MRI. (22,23) The deep part
411 of the repair tissue in the osteochondral defects showed a structure closely resembling that of
412 the healthy control tissue in polarized light microscopy, whereas the chondral defects showed
413 poorly organized tissue in each layer, implying a mechanically weaker tissue structure. These
414 findings substantiate the previous studies that show that the repair tissue originates from the
415 bone marrow (24) and explain the poor outcome of the chondral defects.

416 Although the osteochondral defects showed better repair than chondral defects, the bone voids
417 of the deep osteochondral defects did not heal or even became larger, extending up to 9 mm
418 into the bone, during the 12-month follow-up. Even the smallest 2 mm osteochondral lesions
419 showed bone pathologies at the time of the post mortem analysis (4 of 5 specimens). Frequent
420 cyst formation after a disruption of subchondral bone has been reported in previous equine
421 studies. (18,25) The present study makes no exception: chondral lesions presented with no cysts
422 whereas bone defects were detected in osteochondral lesions of all sizes (2, 4 and 8 mm).

423 The long-term follow-up time of 12 months in this study gives a better understanding of the
424 spontaneous repair capacity of equine carpal joint cartilage than the shorter time periods of
425 previous studies on spontaneous repair. (8,26) Additionally, this study has several
426 methodological benefits, as current state-of-art methods were used in assessing the repair tissue
427 quality. The tissue was evaluated prior to any processing macroscopically and with μ CT and
428 MRI. The outcome of polarized light microscopy reflects the mechanical strength of the repair
429 tissue. (27,28) Finally, the overall quality of the repair tissue was assessed with histological and
430 immunohistochemical techniques. The findings of different methods support each other.

431 There were some limitations in this study. Since defects were created in different sites of the
432 joint, they were subjected to different weight-bearing conditions. (7,8) All defects with the same
433 diameter were, however, located on the same site and thus the comparison between chondral
434 and osteochondral defects is justified. The third carpal bone, where the 4 mm and 8 mm defects
435 were located, bears most weight and is the site in the equine carpus that is most frequently
436 affected by cartilage pathologies. (29) Nonetheless, not even the 2 mm lesions located on the
437 less weight-bearing second carpal bone healed well.

438 Altogether four defects were created in the middle carpal joint of the horses. The combined area
439 of these defects was 94 mm², which might possibly have affected the repair of the individual
440 lesions, although degenerative changes were absent around the lesions or on the articulating
441 surfaces. Further, it is not uncommon to create more defects per joint when using the equine
442 model (30,31). In our study in the carpus, none of the lesions with a diameter of 4 mm (13 mm²)
443 or 8 mm (50 mm²) healed with mature hyaline cartilage. Even the smallest 2 mm in diameter
444 (3 mm²) lesions, which were initially thought to serve as the control lesions with good
445 spontaneous healing showed repair tissue of questionable quality at 12 months.

446 **Conclusion**

447 The horse is a good animal model for cartilage research and, like humans, it has a very limited
448 spontaneous healing capacity. Based on this study, we recommend using 4 mm diameter as the
449 critical size for osteochondral lesions and 2 mm diameter lesion as the critical size for chondral
450 lesions in articular cartilage repair research using the equine carpal joint model.

451

452 **Declaration of Interests**

453 The authors report no conflict of interest. The authors alone are responsible for the content and
454 writing of the article.

455

456 **Funding**

457 This work was supported by the Academy of Finland (Grant #285909) and the Finnish Funding
458 Agency for Innovation Tekes (Grant 3344/31/03).

459

460 **Acknowledgements**

461 The authors wish to thank Outi Kiekara (Department of Anatomy, University of Eastern
462 Finland, Kuopio, Finland) for μ CT and MR imaging. We thank Nora Rauhala (Department of
463 Applied Physics, University of Eastern Finland, Kuopio, Finland) for conducting the ROI
464 analyses on the MRI data and Eija Rahunen (Department of Anatomy, University of Eastern
465 Finland, Kuopio, Finland) for technical assistance with histological sample preparation. The
466 Biomedicum Imaging Unit (Faculty of Medicine, University of Helsinki) is acknowledged for
467 microscopy services and Hannu Kautiainen (Medcare Oy, Äänekoski, Finland) for the
468 statistical analyses.

469

470 **REFERENCES**

- 471 (1) Ahern BJ, Parvizi J, Boston R, Schaer TP. Preclinical animal models in single site cartilage defect
472 testing: a systematic review. *Osteoarthritis Cartilage* 2009 Jun;17(6):705-713.
- 473 (2) Moran CJ, Ramesh A, Brama PA, O'Byrne JM, O'Brien FJ, Levingstone TJ. The benefits and
474 limitations of animal models for translational research in cartilage repair. *J Exp Orthop* 2016 Dec;3(1):1-
475 015-0037-x. Epub 2016 Jan 6.
- 476 (3) Chu CR, Szczodry M, Bruno S. Animal models for cartilage regeneration and repair. *Tissue Eng*
477 *Part B Rev* 2010 Feb;16(1):105-115.
- 478 (4) Malda J, Benders KE, Klein TJ, de Grauw JC, Kik MJ, Hutmacher DW, et al. Comparative study of
479 depth-dependent characteristics of equine and human osteochondral tissue from the medial and lateral
480 femoral condyles. *Osteoarthritis Cartilage* 2012 Oct;20(10):1147-1151.
- 481 (5) Hurtig MB, Fretz PB, Doige CE, Schnurr DL. Effects of lesion size and location on equine articular
482 cartilage repair. *Can J Vet Res* 1988 Jan;52(1):137-146.
- 483 (6) Bernhard JC, Vunjak-Novakovic G. Should we use cells, biomaterials, or tissue engineering for
484 cartilage regeneration? *Stem Cell Res Ther* 2016 Apr 18;7(1):56-016-0314-3.
- 485 (7) Convery FR, Akeson WH, Keown GH. The repair of large osteochondral defects. An experimental
486 study in horses. *Clin Orthop Relat Res* 1972 Jan-Feb;82:253-262.
- 487 (8) McIlwraith CW, Fortier LA, Frisbie DD, Nixon AJ. Equine Models of Articular Cartilage Repair.
488 *Cartilage* 2011 Oct;2(4):317-326.
- 489 (9) McIlwraith CW, Frisbie DD, Kawcak CE. The horse as a model of naturally occurring osteoarthritis.
490 *Bone Joint Res* 2012 Nov 1;1(11):297-309.
- 491 (10) Viren T, Huang YP, Saarakkala S, Pulkkinen H, Tiitu V, Linjama A, et al. Comparison of
492 ultrasound and optical coherence tomography techniques for evaluation of integrity of spontaneously
493 repaired horse cartilage. *J Med Eng Technol* 2012 Apr;36(3):185-192.
- 494 (11) Kulmala KA, Pulkkinen HJ, Rieppo L, Tiitu V, Kiviranta I, Brunott A, et al. Contrast-Enhanced
495 Micro-Computed Tomography in Evaluation of Spontaneous Repair of Equine Cartilage. *Cartilage* 2012
496 Jul;3(3):235-244.
- 497 (12) Rautiainen J, Lehto LJ, Tiitu V, Kiekara O, Pulkkinen H, Brunott A, et al. Osteochondral repair:
498 evaluation with sweep imaging with fourier transform in an equine model. *Radiology* 2013
499 Oct;269(1):113-121.
- 500 (13) Rieppo J, Hallikainen J, Jurvelin JS, Kiviranta I, Helminen HJ, Hyttinen MM. Practical
501 considerations in the use of polarized light microscopy in the analysis of the collagen network in
502 articular cartilage. *Microsc Res Tech* 2008 Apr;71(4):279-287.

- 503 (14) Muhonen V, Salonius E, Haaparanta AM, Jarvinen E, Paatela T, Meller A, et al. Articular cartilage
504 repair with recombinant human type II collagen/poly lactide scaffold in a preliminary porcine study. *J*
505 *Orthop Res* 2015 Nov 17.
- 506 (15) Schindelin J, Arganda-Carreras I, Frise E, Kaynig V, Longair M, Pietzsch T, et al. Fiji: an open-
507 source platform for biological-image analysis. *Nat Methods* 2012 Jun 28;9(7):676-682.
- 508 (16) McIlwraith CW, Frisbie DD, Kawcak CE, Fuller CJ, Hurtig M, Cruz A. The OARSI histopathology
509 initiative - recommendations for histological assessments of osteoarthritis in the horse. *Osteoarthritis*
510 *Cartilage* 2010 Oct;18 Suppl 3:S93-105.
- 511 (17) Riddle WE, Jr. Healing of articular cartilage in the horse. *J Am Vet Med Assoc* 1970 Dec
512 1;157(11):1471-1479.
- 513 (18) Frisbie DD, Trotter GW, Powers BE, Rodkey WG, Steadman JR, Howard RD, et al. Arthroscopic
514 subchondral bone plate microfracture technique augments healing of large chondral defects in the radial
515 carpal bone and medial femoral condyle of horses. *Vet Surg* 1999 Jul-Aug;28(4):242-255.
- 516 (19) Vachon A, Bramlage LR, Gabel AA, Weisbrode S. Evaluation of the repair process of cartilage
517 defects of the equine third carpal bone with and without subchondral bone perforation. *Am J Vet Res*
518 1986 Dec;47(12):2637-2645.
- 519 (20) Vachon AM, McIlwraith CW, Trotter GW, Norrdin RW, Powers BE. Morphologic study of repair
520 of induced osteochondral defects of the distal portion of the radial carpal bone in horses by use of glued
521 periosteal autografts [corrected. *Am J Vet Res* 1991 Feb;52(2):317-327.
- 522 (21) Hunziker EB. The elusive path to cartilage regeneration. *Adv Mater* 2009 Sep 4;21(32-33):3419-
523 3424.
- 524 (22) Nieminen MT, Nissi MJ, Mattila L, Kiviranta I. Evaluation of chondral repair using quantitative
525 MRI. *J Magn Reson Imaging* 2012 Dec;36(6):1287-1299.
- 526 (23) Nissi MJ, Toyras J, Laasanen MS, Rieppo J, Saarakkala S, Lappalainen R, et al. Proteoglycan and
527 collagen sensitive MRI evaluation of normal and degenerated articular cartilage. *J Orthop Res* 2004
528 May;22(3):557-564.
- 529 (24) Shapiro F, Koide S, Glimcher MJ. Cell origin and differentiation in the repair of full-thickness
530 defects of articular cartilage. *J Bone Joint Surg Am* 1993 Apr;75(4):532-553.
- 531 (25) Kold SE, Hickman J, Melsen F. An experimental study of the healing process of equine chondral
532 and osteochondral defects. *Equine Vet J* 1986 Jan;18(1):18-24.
- 533 (26) Frisbie DD, Lu Y, Kawcak CE, DiCarlo EF, Binette F, McIlwraith CW. In vivo evaluation of
534 autologous cartilage fragment-loaded scaffolds implanted into equine articular defects and compared
535 with autologous chondrocyte implantation. *Am J Sports Med* 2009 Nov;37 Suppl 1:71S-80S.
- 536 (27) Vasara AI, Hyttinen MM, Lammi MJ, Lammi PE, Langsjo TK, Lindahl A, et al. Subchondral bone
537 reaction associated with chondral defect and attempted cartilage repair in goats. *Calcif Tissue Int* 2004
538 Jan;74(1):107-114.

- 539 (28) Julkunen P, Harjula T, Iivarinen J, Marjanen J, Seppanen K, Narhi T, et al. Biomechanical,
540 biochemical and structural correlations in immature and mature rabbit articular cartilage. *Osteoarthritis*
541 *Cartilage* 2009 Dec;17(12):1628-1638.
- 542 (29) Palmer JL, Bertone AL, Litsky AS. Contact area and pressure distribution changes of the equine
543 third carpal bone during loading. *Equine Vet J* 1994 May;26(3):197-202.
- 544 (30) Hurtig M, Pearce S, Warren S, Kalra M, Miniaci A. Arthroscopic mosaic arthroplasty in the equine
545 third carpal bone. *Vet Surg* 2001 May-Jun;30(3):228-239.
- 546 (31) Nixon AJ, Rickey E, Butler TJ, Scimeca MS, Moran N, Matthews GL. A chondrocyte infiltrated
547 collagen type I/III membrane (MACI(R) implant) improves cartilage healing in the equine
548 patellofemoral joint model. *Osteoarthritis Cartilage* 2015 Apr;23(4):648-660.
- 549